Arab J Geosci (2016) 9:419
DOI 10.1007/s12517-016-2439-1

ORIGINAL PAPER

Land cover change dynamics mapping and predictions using EO data and a GIS-cellular automata model: the case of Al-Baha region, Kingdom of Saudi Arabia

Shereif H. Mahmoud[1] · **A. A. Alazba**[1]

Received: 23 September 2015 / Accepted: 15 March 2016

Abstract The present study designed to monitor and predict land cover change (LCC) in addition to characterizing LCC and its dynamics over Al-Baha region, Kingdom of Saudi Arabia, by utilizing remote sensing and GIS-cellular automata model (Markov-CA). Moreover, to determine the effect of rainwater storage reservoirs as a driver to the expansion of irrigated cropland. Eight Landsat 5/7 TM/ETM images from 1975 to 2010 were analyzed and ultimately utilized in categorizing LC. The LC maps classified into four main classes: bare soil, sparsely vegetated, forest and shrub land, and irrigated cropland. The quantification of LCC for the analyzed categories showed that bare soil and sparsely vegetated was the largest classes throughout the study period, followed by forest, shrubland, and irrigated cropland. The processes of LCC in the study area were not constant, and varied from one class to another. There were two stages in bare soil change, an increase stage (1975–1995) and decline stage (1995–2010), and the construction of 25 rainwater-harvesting dams in the region was the turning point in bare soil change. The greatest increase was observed in irrigated cropland after 1995 in the expense of the other three categories as an effect of extensive rainwater harvesting practices. Losses were evident in forest and shrubland and sparsely vegetated land during the first stage (1975–1995) with 5.4 and 25.6 % of total area in 1995, while in 1975, they covered more than 13.8 and 32.7 % of total area. During the second stage (1995–2010), forest and shrubland witnessed a significant increase from 1569.17 km^2 in 1975 to 1840.87 km^2 in 2010. Irrigated cropland underwent the greatest growth (from 422.766 km^2 in 1975 to 1819.931 km^2 in 2010) during the entire study period, and this agriculture expansion reached its zenith in the 2000s. Markov-CA simulation in 2050 predicts a continuing upward trend in irrigated cropland and forest and shrubland areas, as well as a downward trend in bare soil and sparsely vegetated areas; the spatial distribution prediction indicates that irrigated cropland will expand around reservoirs and the mountain areas. The validation result showed that the model successfully identified the state of land cover in 2010 with 97 % agreement between the actual and projected cover. The output of this study would be useful for decision makers and LC/land use planners in Saudi Arabia and similar arid regions.

Keywords Remote sensing · Land cover change (LCC) · GIS-cellular automata model · Markov model · GIS

Introduction

Land cover changes describe differences in the area occupied by cover types through time. Both losses and gains are included. Land cover change (LCC) analyses and projection are one of the main tools to evaluate ecosystem change and resultant environmental implications at various temporal and spatial scales (Lambin 1997; Zhang et al. 2011; Tong et al. 2012). Despite its relevance, quantitative data describing where, when, and how changes occurs are incomplete or inexact (Turner et al. 1993). Thus, research on this subject is important in order to understand patterns of LCC change in relation to human activities and natural processes at different spatial and temporal scales. Land cover changes especially those caused by human activities are one of the most important components of global environmental change with impacts possibly greater

✉ Shereif H. Mahmoud
eng.shereif1@hotmail.com; shmahmoud@ksu.edu.sa

[1] Alamoudi Water Research Chair, King Saud University, PO Box: 2460,, Riyadh 11451, Saudi Arabia

Published online: 03 May 2016

than the other types of global changes (Turner et al. 1994; Jensen 2005).

Recently, the issue of LCC has become a core component of research in many international and interdisciplinary studies (Turner et al. 1994, 2007; Jensen 2005; Li et al. 2008, 2009; Petropoulos et al. 2010; Roy et al. 2014). Changes in land use and land cover have been directly linked to biodiversity loss, transborder migration, environmental refuge, food security, urbanization, soil quality and runoff, and sedimentation rates, among other processes (López et al. 2001; Dunjó et al. 2003; Heistermann et al. 2006; Milesi et al. 2005; Wang et al. 2009; Wilson and Weng 2011; Shoyama et al. 2014). The balance between human activities and natural processes could decide future conservation planning over large areas of the planet. Therefore, it is important to quantify the effect of human-driven conversion of natural processes into disturbed or human-dominated environments (Satake and Rudel 2007; Clement et al. 2009; Redo et al. 2009; Marey-Pérez and Rodríguez-Vicente 2009; Kashaigili and Majaliwa 2010).

Remote sensing and geographic information systems (GIS) have been widely applied to identify and analyze land use, LCC, and multitemporal data that used to quantify the type, amount, and location of LCC (Eastman and Fulk 1993; Longley 2005; Lu et al. 2004; Long et al. 2007; Haregeweyn et al. 2012). Various change detection techniques have been developed to identify the extent and locations of land use and cover changes, such as principal component analysis (PCA), band differencing, band ratioing, and postclassification comparison (Lu et al. 2004; Ridd and Liu 1998; Petropoulos et al. 2011; Petropoulos et al. 2012; Srivastava et al. 2012; Petrosillo et al. 2013; Borrelli et al. 2013; Teferi et al. 2013; Elatawneh et al. 2014). A historically common method of predicting the change among various categorical states is the application of Markov modeling (Pontius and Malanson 2005).

The combination of cellular automata (CA) with Markov modeling is the most common methods to present assessments of LUCC (Zhang et al. 2009). As CA models not only offers a new way of thinking for dynamic process modeling, but it also provides a laboratory for testing the decision-making processes. CA is one of the most common methods of predicting LCC due to its capabilities to address the complex problems based on simple transition rules in comparison with traditional approaches based on differential or difference equations (Baker 1989). In addition, CA is the preferred model for many researchers due to its computational efficiency (White et al. 1997), because it has the ability to perform spatial dynamics, and time explicitly (Wagner 1997).

CA is well suited to represent geographic processes due to the similarities between a two-dimensional lattice and a raster grid (Longley and Batty 1996; Clarke and Gaydos 1998; Clarke et al. 1997; Torrens 2003). CA has been used intensively in modeling land use/cover change and prediction (Brown et al. 2000; Myint and Wang 2006; Marshall and Randhir 2008; Kamusoko et al. 2009; Mitsova et al. 2011; Guan et al. 2011; Nouri et al. 2011; Huishi et al. 2012; Al-Sharif and Pradhan 2013; Liu et al. 2014; Huang et al. 2014; Yagoub and Al-Bizreh 2014).

Myint and Wang (2006) used an integration of Markov chain analysis and a CA approach to predict land use/land cover change in Norman, OK, USA. This study revealed that the combination of Markov and CA was effective in projecting future land use/land cover, since the overall accuracy was 86 %, which is higher than the standard acceptable accuracy of 85 % (Anderson et al. 1976; Townshend 1981). More recently, Kashaigili and Majaliwa (2010) conducted a study to investigate long-term and seasonal changes that have occurred in the Malagarasi River watershed in Tanzania, Africa, through human activities from 1984 and 2001. These authors reported that there was a significant change in land use and cover within the 18-year period. The principal drivers for the changes were found to include fire, cultivation along rivers and lakeshores, overgrazing, poor law enforcement, insufficient knowledge of environmental issues, increasing poverty, deforestation, and population growth. Another study conducted by Shoyama et al. (2014) in Japan revealed that if no conservation measures were implemented and even if the timber and agricultural industries remained small until 2060, supporting and provisioning services would decline due to less land management. Mitsova et al. (2011) developed Markov-CA model to integrate protection of environmentally sensitive areas into urban growth projections at a regional scale. The modeling approach applies CA, Markov probabilities, and multicriteria evaluation to simulate five land cover classes simultaneously. Similarly, Nouri et al. (2011) explored the potential of CA in planning support tools for analysis of temporal changes and spatial distribution of urban land uses in Anzali-Iran and discussed its ability to simulate future land use. Huishi et al. (2012) investigated the LCC in Hulun Buir Grassland of China by integrating the Markov process into the CA mode. These authors reported that in comparison with GIS and statistical methods, the Markov-CA model is fast, accurate, and real-time (Guan et al. 2011; Huang et al. 2014). In addition, the Markov-CA model is relatively easy to use. Yagoub and Al-Bizreh (2014) coupled remotely sensed imagery with CA models to predict LC in Al Ain City, Emirate of Abu Dhabi. This study demonstrates that integrating remote sensing with CA models is useful, where there is no available data for decision makers or planners.

The present study is the first analysis and estimation of LCC in Kingdom of Saudi Arabia (KSA) caused by human activities and natural processes at different spatial and temporal scales. The study of LCC in KSA is gaining importance in the last years for several reasons. First, the KSA government wants to decrease pressures on natural resources, particularly forests and to assess the effectiveness of current conservation

projects, including water harvesting and recharge structure in order to provide recommendations for future conservation plans. Second, the study of LCC dynamics could help decision makers to launch the balance between LCC and conservation policies that consider both economic development and environmental management.

The main objective of the present study was to monitor and predict LCC over Al-Baha region, KSA, in addition to characterizing LCC and its dynamics by utilizing remote sensing, GIS techniques, and determine the effect of rainwater storage reservoirs as a driver to the expansion of irrigated cropland. By assessing LCC within the study period, we can observe how environmental policies affect land management in KSA. The subobjectives in this study included the following:

- To identify LCC at eight periods between 1975 and 2010 using remotely sensed data and Markov model
- To quantify LCC through transition matrices and to predict LCC in 2050 and its environmental impacts using CA and a Markov model
- To identify the impact of human activities on the ecosystem services

Material and methods

Study area

Al-Baha Province is situated in Hejaz, western part of the KSA (41° 42 E, 19° 20 N) between Makah and Asser (Fig. 1). This province is the smallest in KSA including 12, 000 km^2. Al-Baha Province was selected to implement this study due to its considerable divergence in its topography and climate. The study periods selected was selected based on environmental problems and concerns indicated in the study area such as reservoir construction and deforestation. The climate, in general, falls in the arid zone classification. Relative humidity varies between 52 and 67 % with temperatures ranging between 12 and of 23 °C as minimum and maximum, respectively. Rainfall is much higher than KSA average, yet it ranges between 200 and 600 mm/year (Mahmoud et al. 2014a, b, c; Mahmoud 2014).

Land cover classification and accuracy assessment

Eight Landsat 5/7 TM/ETM images were obtained for the years 1975, 1980, 1985, 1990, 1995, 2000, 2005, and 2010 (Table 1). These images were selected based on phenology and scene quality (cloudiness and haze); optimal time periods for discriminating land cover types were also identified for each Landsat path-row footprint, and each proposed land cover mapping zone. Then, the selected images were radiometrically and geometrically calibrated and smoothed using a weighted multiple regression technique. Finally, these images were incorporated with filed survey data from the specified region and ultimately utilized in categorizing land cover (LC). Erdass Imagine software 2013 was used to mosaic the collected satellite images. After geometric corrections, Iso Cluster unsupervised classification and maximum likelihood classification method (Richards 1999) were used for the unsupervised and supervised classification. These methods combine the functionalities of the Iso Cluster and maximum likelihood classification tools. It outputs a signature file. The resulting

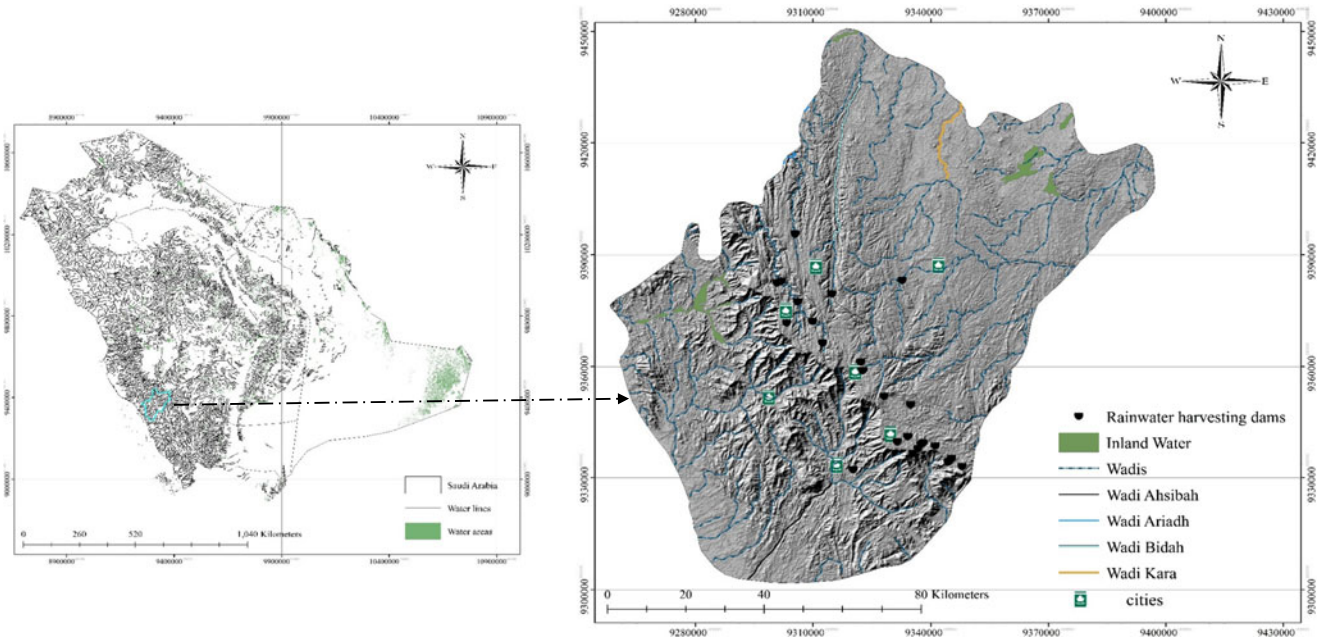

Fig. 1 Location map of the study area

Table 1 Remote sensing data used for the study

Images used for the study	Resolution (m)	Date of acquisition	Product type (cloud cover %)
Landsat 5 TM "Band 1–7"	30	23 June1975	L1T[a] (0 %)
Landsat 5 TM "Band 1–7"	30	11 August 1980	L1T[a] (0 %)
Landsat 5 TM "Band 1–7"	30	2 August 1985	L1T[a] (0 %)
Landsat 5 TM "Band 1–7"	30	9 November 1990	L1T[a] (0 %)
Landsat 5 TM "Band 1–7"	30	2 August 1995	L1T[a] (0 %)
Landsat 7 ETM+ "Band 1–8"	30	27 May 2000	L1T[a] (0 %)
Landsat 7 ETM+ "Band 1–8"	30	5 March 2005	L1T[a] (0 %)
Landsat 7 ETM+ "Band 1–8"	15	7 July 2010	L1T[a] (0 %)

[a] Level 1T (L1T) (precision and terrain corrected data) provides systematic radiometric accuracy, geometric accuracy by incorporating ground control points, while also employing a digital elevation model (DEM) for topographic accuracy

signature file from this tool can be used as the input for another classification tool, such as maximum likelihood classification, for greater control over the classification parameters. The maximum likelihood classification has been widely used in many classification applications (Vorovencii and Muntean 2012). The method is based on the likelihood that each pixel belongs to a particular class. The basic theory assumes that these likelihoods are equal for all classes and that input bands are evenly distributed. In the present study, training samples collected during field survey to create spectral signatures (i.e., reflectance values) for the supervised classification to identify what the cluster represents (e.g., water, bare earth, dry soil, etc.). Spatiotemporal mapping includes quantitative time series analysis and transformation of LC classes using remotely sensed images for each timestamp. In addition, the classification accuracy of the classified images was determined by simple random patterns. The simple random pattern is the most common approach and provides an equivalent probability of sampling over the entire study area with no operator bias. A detailed flowchart for the methodology used in this study is presented in Fig. 2.

Modeling land cover changes and dynamics

Change detection is the process of identifying differences in LC and land use, among multiple remotely sensed data of an area. From previous studies, various change detection techniques have been developed and used with satellite imagery, for example, principal component analysis, image differencing, spectral vector analysis, and postclassification (Abuelgasim et al. 1999; Jensen 2005). Land Change Modeler for ecological sustainability are into integrated software developed by IDRISI Selva for analyzing LCCs. LCC model tools support the analysis of the land use changes. Use of such and the support needed for planning and policy-making. In this study, LCC and dynamics were determined using the Land Change Modeler (LCM) in IDRISI 17 (Selva Edition). The results were evaluated using a change detection

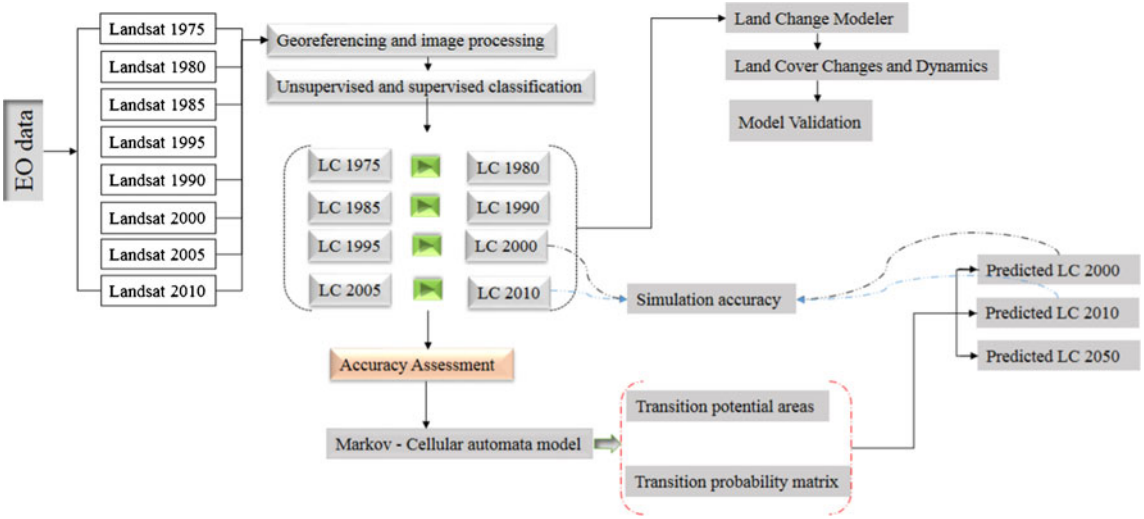

Fig. 2 Flowchart of the methodology used in this study

matrix, with detailed "from-to" information then extracted from the matrix. The area percentages of three classified images were first plotted by category to observe the trends in LCC. Then, the earlier and later classified images in the LCM change analysis panel were used. This panel provided gain and loss graphs and net change graphs for each temporal period by category for calculation of the area and percentage of change. Next, the additional from-to information was computed using the crosstab module, which provided a cross-classification image showing the locations of the categories in the earlier image that were the same as those in the second image, and vice versa. Finally, the earlier classified images and cross-classification images for each period were used to determine the relative frequency of the different land cover categories occurring in areas of transition. Transition probability and the quantity of future changes were modeled through Markov chain analysis. The output from the transition prediction was the LC transition probability in 2050.

Markov-cellular automata model

This study employs a coupled Markov-CA model that integrates GIS software to model LCCs and spatial distribution in the future. A Markovian process is one in which the state of a system at time t_2 can be predicted by the state of the system at time t_1 given a matrix of transition probabilities from each land cover class to every other cover class. Markov-CA is a combined CA/Markov change land cover prediction procedure that adds an element of spatial contiguity as well as knowledge of the likely spatial distribution of transitions to Markov change analysis. One of the basic spatial elements that underly the dynamics of many change events is proximity: areas will have a higher tendency to change to a class when they are near existing areas of the same class. These can be very effectively modeled using CA. A cellular automaton is a cellular entity that independently varies its state based on its previous state and that of its immediate neighbors according to a specific rule. Clearly, there is a similarity here to a Markovian process. The only difference is the application of a transition rule that depends not only upon the previous state but also upon the state of the local neighborhood. In this study, Markov module was used to create a transition probability matrix for each subperiod. The output of the Markov chain analysis is the following output:

1. A transition probability matrix. This expresses the likelihood that a pixel of a given class will change to any other class or stay the same in the next time period.
2. A transition areas matrix. This expresses the total area expected to change in the next time-period.
3. A set of conditional probability images (transition maps)—one for each land cover class. These maps express the probability that each pixel will belong to the designated class in the next time period.

Computation of the transition probability matrix/transition potential areas

The Markov chain analysis was used to compute transition probabilities based on the Landsat derived land cover maps for 1975, 1980, 1985, 1990, 1995, 2000, 2005, and 2010. Seven transition matrices were constructed from the cross-tabulation of the land cover maps. The time intervals used for calibration were 5 years for each transition matrix. Consequently, transition probabilities were normalized to annual time steps as demonstrated by Pastor et al. (1993) in order to take account of differences in the lengths of the two time periods. The original transition probability matrices for each land cover type need to be defined prior to Markov process. Its mathematical expression is as follows:

$$P = \left(P_{ij}\right) = \begin{bmatrix} P_{11} & P_{12}\cdots\ldots & P_{1n} \\ P_{21} & P_{22}\cdots\ldots & P_{2n} \\ & \cdots & \\ P_{n1} & P_{n2}\cdots\ldots & P_{nn} \end{bmatrix} \quad (1)$$

In the above matrix, P_{ij} is the transformation probability of the ith type land into the jth type land from prophase to telophase and n is the land cover type of studied area. P_{ij} should meet the following conditions:

$$0 \le P_{ij} \le (i,j) = (1,2,3,4,..,n) \quad (1.1)$$

$$\sum\nolimits_{i=1}^{n} P_{ij} = 1(i,j = 1,2,3,4,..,n) \quad (1.2)$$

According to the non-after effect of Markov process and probability formulae of Bayes condition, forecast model of Markov is obtained:

$$P_n = P_{(n-1)}P_{ij} \quad (2)$$

P_n is the state probability of any times, and $P_{(n-1)}$ is the preliminary state probability.

Map algebra applied to land cover map to calculate transition probability values in the period between each two maps. Successively, transition matrices of land cover types in each period were obtained by using a Markov model as shown in Table 2. The potential power of transition was determined which LC classes were the major drivers of LC dynamics in the study area for each temporal period. After the major transitions was created, the earlier classified images and cross-classification images of each period were used to determine the relative frequency of different LC categories that occurred within the areas of transitions.

Table 2 Land cover transitional probabilities of each subperiod and the full period 1975–2010

1975–1980 Markov matrix[a]					
Code	Land cover class	Bare soil	Sparsely vegetated	Forest and shrubland	Irrigated cropland
1	Bare soil	0.1814	0.1062	0.0382	0.009
2	Sparsely vegetated	0.0465	0.0396	0.0132	0.0032
3	Forest and shrubland	0.0285	0.0255	0.0159	0.0032
4	Irrigated cropland	0.018	0.0089	0.0085	0.0051
1980–1985 Markov matrix[a]					
Code	Land cover class	Bare soil	Sparsely vegetated	Forest and shrubland	Irrigated cropland
1	Bare soil	0.2602	0.0345	0.0134	0.0031
2	Sparsely vegetated	0.0459	0.0349	0.0164	0.0029
3	Forest and shrubland	0.0219	0.0241	0.0238	0.0088
4	Irrigated cropland	0.0069	0.0090	0.0195	0.0257
1985–1990 Markov matrix[a]					
Code	Land cover class	Bare soil	Sparsely vegetated	Forest and shrubland	Irrigated cropland
1	Bare soil	0.2511	0.0704	0.0426	0.0137
2	Sparsely vegetated	0.0472	0.0237	0.0260	0.0205
3	Forest and shrubland	0.0111	0.0051	0.0085	0.0196
4	Irrigated cropland	0.0017	0.0009	0.0016	0.0072
1990–1995 Markov matrix[a]					
Code	Land cover class	Bare soil	Sparsely vegetated	Forest and shrubland	Irrigated cropland
1	Bare soil	0.3040	0.0521	0.0057	0.0007
2	Sparsely vegetated	0.0655	0.0516	0.0209	0.0033
3	Forest and shrubland	0.0060	0.0095	0.0107	0.0033
4	Irrigated cropland	0.0024	0.0041	0.0070	0.0041
1995–2000 Markov matrix[a]					
Code	Land cover class	Bare soil	Sparsely vegetated	Forest and shrubland	Irrigated cropland
1	Bare soil	0.2915	0.0770	0.0077	0.0034
2	Sparsely vegetated	0.0623	0.0422	0.0097	0.0049
3	Forest and shrubland	0.0068	0.0163	0.0077	0.0053
4	Irrigated cropland	0.0020	0.0056	0.0044	0.0041
2000–2005 Markov matrix[a]					
Code	Land cover class	Bare soil	Sparsely vegetated	Forest and shrubland	Irrigated cropland
1	Bare soil	0.2908	0.0288	0.0029	0.0009
2	Sparsely vegetated	0.0497	0.0246	0.0019	0.0002
3	Forest and shrubland	0.0306	0.0384	0.0061	0.0008
4	Irrigated cropland	0.0087	0.0273	0.0252	0.0141
2005–2010 Markov matrix[a]					
Code	Land cover class	Bare soil	Sparsely vegetated	Forest and shrubland	Irrigated cropland
1	Bare soil	0.2368	0.0275	0.0126	0.0033
2	Sparsely vegetated	0.0444	0.0242	0.0201	0.0052
3	Forest and shrubland	0.0262	0.0182	0.0284	0.0160
4	Irrigated cropland	0.0160	0.0064	0.0148	0.0508

[a] Values are probabilities of transition

Future scenarios

In order to predict future LC in the study area, an analysis was conducted based on the annualized transition matrices, assuming that the LCC follows a Markovian dynamic—i.e., future scenarios are explored using Markovian transition models, considering trends observed in land cover changes within the study area. The transition probability matrix and the transition areas record the number of cells, or pixels that are expected to change from each land cover class to each other land cover class over the next time period. This matrix was generated by multiplication of each column in the

transition probability matrix by the number of cells of corresponding land cover in the later image. Afterward, the Markov-CA model was applied to predict future LCCs using the following steps:

1. Construction of CA filter: The module uses a 5 × 5 mean filter to achieve this contiguity constraint. By filtering a Boolean mask of the each land cover class, the mean filter yields a value of 1 when it is entirely within the existing class and 0 when it is entirely outside it. This filter has a remarkable influence on the change in the cellular state (Eastman 2001). This result is then multiplied by the suitability image for that class, thereby progressively downweighting the suitability as one moves away from existing instances of that class, and this step is repeated for each class being in the land cover map.
2. Determination of start time and iteration number: Identifying iteration number and time starting point of CA, the Markov-CA model was implemented using a different iteration number starting from one iteration until ten iterations. Based on the land cover pattern in 1975, 1990, and 2000, the CA cycle number is chosen, and the land cover pattern of 2000 and 2010 is simulated to test the simulation accuracy.
3. After validating the model capability to predict the state of land cover in 2000 and 2010, the year 2010 was used as starting point to predict the LCC in 2050.

Model validation

IDRISI Selva supplies a pair of modules to assist in the validation process; these modules were used in the present study to validate the process of LCC. The first is called VALIDATE and provides a comparative analysis based on the kappa index of agreement (Eastman 2001). In addition, overall accuracies and producer's and user's accuracy values for each land cover derived from the error matrix are given in Table 3. Producer's accuracy is calculated by dividing the number of correctly classified pixels in each category by the number of training set pixels used for that category. User's accuracy is computed by dividing the number of correctly classified pixels in each category by the total number of pixels classified in that category. Producer's and user's accuracies in Table 3 indicate how well training set pixels of a given cover type are classified, and the probability that a pixel classified into a given category actually represents that category on the ground, respectively. Kappa is essentially a statement of proportional accuracy, adjusted for chance agreement. However, unlike the traditional kappa statistic, VALIDATE breaks the validation down into several components, each with a special form of kappa or associated statistic (based on the work of Pontius (2000)).

Table 3 Classification accuracy for eight Landsat subscenes

	1975			1980			1985			1990			1995			2000			2005			2010		
Land covers	UA (%)	PA (%)	Kappa	UA (%)	PA (%)	Kappa	UA (%)	PA (%)	Kappa	UA (%)	PA (%)	Kappa	UA (%)	PA (%)	Kappa	UA (%)	PA (%)	Kappa	UA (%)	PA (%)	Kappa	UA (%)	PA (%)	Kappa
Bare soil	80.2	72	0.84	78.6	71.9	0.82	81.6	79.9	0.67	88.9	80	0.77	89	79.9	0.68	87	83.5	0.78	81.4	76.9	0.81	90	88	0.89
Sparsely vegetated	90.4	75.6	0.73	94	96.9	0.75	91.4	89.1	0.85	69.8	79	0.91	87.6	85.8	0.84	94	92.5	0.95	90.3	86.4	0.78	91.2	90.7	0.79
Forest and shrubland	87.6	92.7	0.91	92.5	78.2	0.89	87.3	86	0.96	89.6	93	0.85	93.4	90.1	0.89	89.3	87	0.83	89.6	91.8	0.89	87	100	0.95
Irrigated cropland	95.3	98.4	0.98	98.3	96	1	83.9	98.2	1	97.8	89	1	96.2	91.5	1	100	89	1	99.7	100	0.98	100	97	1
OA	86.52 %		0.86	88.33 %		0.865	87.17 %		0.87	85.90 %		0.88	89.20 %		0.85	90. 3 %		0.89	89.50 %		0.865	93 %		0.91

UA user's accuracy, *PA* producer's accuracy, *OA* overall accuracy

With such a breakdown, for example, it is possible to assess the success with which one is able to specify the location of change versus the quantity of change. The other validation procedure is the relative operating characteristic (ROC). It is used to compare any statement about the probability of an occurrence against a Boolean map, which shows the actual occurrences. It can be useful, for example, in validating modifications to the conditional probability map output from Markov. Note that LOGISTICREG incorporates ROC directly in its output.

Result and discussion

Analysis of LCC and its impacts on ecosystem services

Monitoring of the locations and distributions of LCC constitutes an important step toward establishing links between the policy decisions, regulatory actions, and subsequent LC activities that could result in sustainable management of the environment and highlight risks for future generations. In this study, LC maps for 1975, 1980, 1985, 1990, 1995, 2000, 2005, and 2010 were derived from cloud-free satellite images using ERDAS Imagine 13 software and ArcGIS 10.1 Spatial Analyst. The overall accuracy of the land cover maps for 1975, 1980, 1985, 1990, 1995, 2000, 2005, and 2010 was determined to be 86.52, 88.33, 87.17, 85.9, 89.2, 90.3, 89.5, and 93 %, respectively, where kappa indices for these maps were 0.86, 0.865, 0.87, 0.88, 0.85, 0.89, 0.87, and 0.91, respectively. Table 3 shows a continuous increase to the overall classification accuracy from the images of 1975 to the images of 2010 due to the spatial resolution of various satellite sensors ranges. Furthermore, high-resolution EO data are very helpful for visual interpretation and supervised classification, which allow correcting the misclassified pixels in the Landsat image. These findings are in good agreement with result obtained by Roy et al. (2014).

Arid and semiarid or subhumid zones are characterized by low erratic rainfall, periodic droughts, and different associations of vegetative cover and soils. Vegetation cover is sparse to almost nonexistent. In Arabia, a number of land cover patterns can be observed, and examples are given here for different areas in the Arabian Peninsula. In addition, specific land cover is defined as the observed physical layer including natural and planted vegetation and human constructions, which cover most of the area; however, the major part of the of Saudi Arabia is made up of arid environment, and only a very small portion of the area is covered by vegetation (Hereher et al. 2012; Madugundu et al. 2014; Alqurashi and Kumar 2014). In the present study, land cover classification showed similar pattern with only four main classes: bare soil, sparsely vegetated land, forest and shrubland, and irrigated cropland. The images suggest that LCC have had significant effect on forest and shrubland, which may have affected the ecosystem and natural balance of the study area throughout the entire study period (Fig. 3). The results of LCC analysis identified an increase of irrigated croplands after 1995. The quantification of LCC in the analyzed categories showed that bare soil and sparsely vegetated were the largest classes throughout the study period followed by forest, shrubland, and irrigated cropland. The processes of LCC in the study area were not constant and varied from one class to another. There were two stages in the bare soil change, an increase stage (1975–1995) and decline stage (1995–2010), and the construction of 25 rainwater reservoirs in the region were the transition point of bare soil change. The greatest increase was observed in irrigated cropland after 1995 at the expense of the other three categories as an effect of extensive irrigation from these reservoirs.

The extent of the land cover distribution throughout the study period (1975–2010) is presented in Table 4. There were two stages in the bare soil change, an increase stage (1975–1995) and decline stage (1995–2010). A continued increase in bare soil was observed during the first stage, increasing from 5684 km^2 in 1975 to 7859 km^2 in 2000; the second stage showed a decline in areas occupied by bare soil from more than 7859 km^2 in 2000 to less than 5804 km^2 in 2010—more than 200 km^2 decline. Similarly, there was a general decline trend in forest and shrubland, which declined from 1569 km^2 in 1975 to 747 km^2 in 2000, followed by an increase to 1840 km^2 in 2010 because of conservation efforts. Sparsely vegetated land followed a three-stage trend, a decline stage, declining from 3731 km^2 in 1975 to 2071 km^2 in 1985, followed by an increase in area occupied by sparsely vegetated land increasing to 2924 km^2 in 1995. The third stage showed a significant decline in sparsely vegetated land from 2924 km^2 in 1995 to 1942 km^2 in 2010. However, this period also showed a substantial increase in irrigated cropland relative to 1995 (1819 km^2 vs 364 km^2). Table 5 indicates LCC in the study area for each subperiod and the full period 1975–2050 in percentage terms.

Twenty-five reservoirs were constructed within the study area during the period of analyses, 70 % of which were constructed to recharge groundwater supplies. Construction of these reservoirs were initiated to restore groundwater resources had been depleted. Groundwater depletion over the years has reduced regional agricultural production because groundwater wells are the main source of water. The surveys revealed that only 4 % of the reservoirs are used for irrigation and other uses and 12 % for flood control. In addition, 14 % of the dams were established for drinking purposes in areas in which desalinated water is difficult to obtain. In general, the main purpose of the existing dams in the study area is to recharge groundwater supplies in support of the agricultural sector, as groundwater is the main source of water for irrigation in KSA (Mahmoud and Alazba 2014). The change in natural drainage patterns by the construction of reservoirs

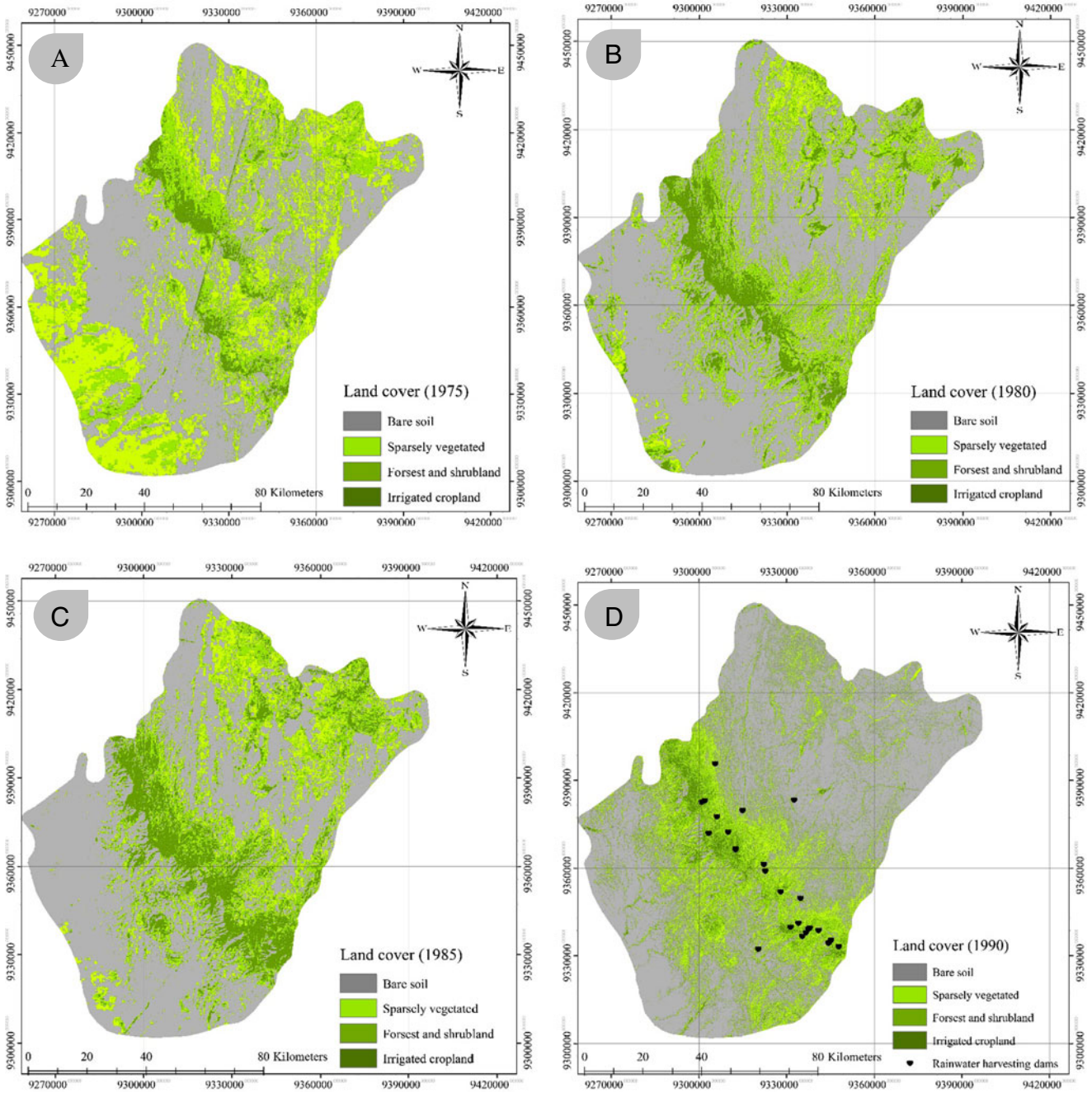

Fig. 3 Classification and dynamics of land cover changes in the study region based on time series EO images from 1975, 1980, 1985, 1990, 1995, 2000, 2005, and 2010

affecting the land cover in the study area during the research period is clearly evident in Fig. 4. In 1990, there was limited human interaction with the environment and forest cover dominated the area. However, conditions changed substantially thereafter, and following the reservoir construction, no water drained into the streams or forestland, impacting native vegetation cover. Overall, the effects of LCC on the hydrology of the study area can be summarized as follows: (1) substantially changing the area's ecosystems, as human alteration of land cover from natural vegetation to other uses typically results in loss, degradation, and fragmentation, all of which usually have devastating effects on the biodiversity of the region (such impacts reflect on the Afrotropical biodiversity of the region; (2) loss of forest cover; and (3) decreased surface runoff values, as the change in drainage due construction of rainwater retention dams affected the land cover type in the study area. These findings are in good agreement with result obtained by Li et al. (2009).

The LCC map (from-to) in this study (Figs. 5 and 6) were produced using the combined approach and revealed

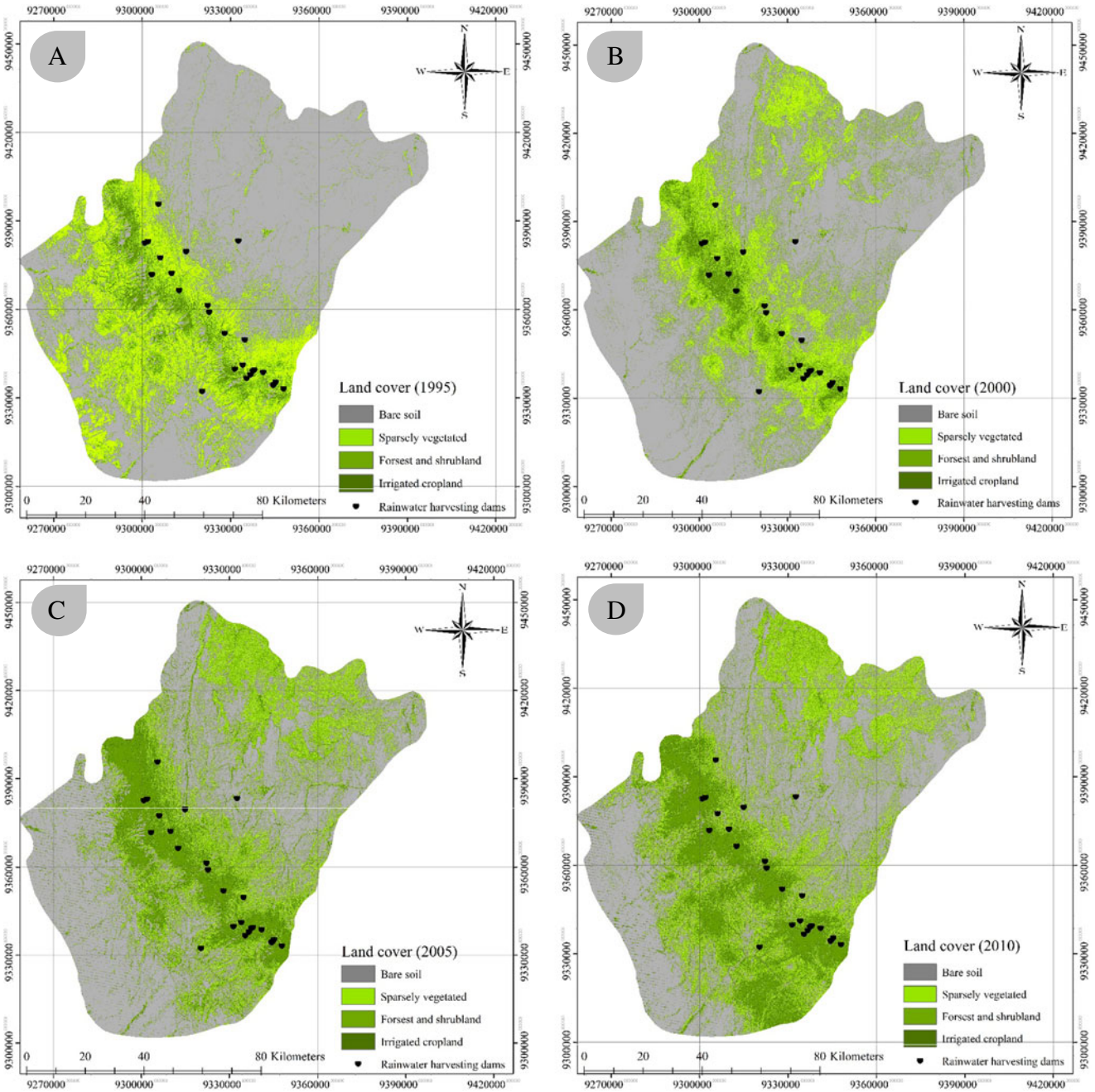

Fig. 3 (continued)

extensive increases in irrigated cropland at the expense of forest, shrubland, and grassland, and bare soil. Based on from-to images, losses were evident in forest and shrubland and sparsely vegetated land during the first stage (1975–1995) with 5.4 and 25.6 % of the total area in 1995, whereas in 1975, these LC were 13.8 and 32.7 % of the total area. During the second stage (1995–2010), forest and shrubland witnessed a significant increase from 1569.17 km^2 in 1975 to 1840.87 km^2 in 2010 (an increase of 16.1 % of the total area in 2010). Irrigated cropland underwent the greatest growth (from 422.766 km^2 in 1975 to 1819.931 km^2 in 2010) during the entire study period and this agriculture expansion reached its peak in the 2000s.

The effects of changing LC patterns on water resources and environment create social and political tensions at the local and national levels worldwide (YAO et al. 2014). In the Al-Baha region of KSA, for example, the shift toward agriculture has generated a number of changes in the structure and function of ecosystems, resulting in an overall degradation of the ecological services provided by region's natural ecosystems. In addition, the forests of the Al-Baha

Table 4 Area measurements of land-cover within Al-Baha province for each subperiod and the full period 1975–2050

	1975		1980		1985		1990		1995		2000		2005		2010		2050	
Code	Area (km^2)	Area (%)	Area (km^2)	Area (%)	Area (km^2)	Area (%)	Area (km^2)	Area (%)	Area (km^2)	Area (%)	Area (km^2)	Area (%)	Area (km^2)	Area (%)	Area (km^2)	Area (%)	Area (km^2)	Area (%)
1	5684.035	0.498	6934.683	0.608	6443.257	0.565	7822.500	0.686	7507.843	0.658	7859.780	0.689	6697.158	0.587	5804.061	0.509	2203.956	0.193
2	3731.231	0.327	2122.338	0.186	2071.682	0.182	2430.230	0.213	2924.109	0.256	2465.470	0.216	1580.567	0.139	1942.367	0.170	988.387	0.087
3	1569.169	0.138	1511.956	0.133	1629.314	0.143	916.350	0.080	610.842	0.054	747.010	0.065	1570.760	0.138	1840.870	0.161	1547.438	0.136
4	422.766	0.037	838.210	0.073	1263.059	0.111	236.300	0.021	364.523	0.032	333.120	0.029	1558.701	0.137	1819.931	0.160	6668.374	0.585

Table 5 Detected land cover gains and losses in Al-Baha province, 1975–1980, 1980–1985, 1985–1990, 1990–1995, 1995–2000, 2000–2005, 2005–2010, and 2010–2050

	1975–1980		1980–1985		1985–1990		1990–1995		1995–2000		2000–2005		2005–2010		2010–2050	
Code	Change (km^2)	Change (%)	Change (km^2)	Change (%)	Change (km^2)	Change (%)	Change (km^2)	Change (%)	Change (km^2)	Change (%)	Change (km^2)	Change (%)	Change (km^2)	Change (%)	Change (km^2)	Change (%)
1	−1250.65	−22.00	491.43	7.09	−1379.24	−21.41	314.66	4.02	−351.94	−4.69	1162.62	14.79	893.10	13.34	3600.11	62.03
2	1608.89	43.12	50.66	2.39	−358.55	−17.31	−493.88	−20.32	458.64	15.68	884.90	35.89	−361.80	−22.89	953.98	49.11
3	57.21	3.65	−117.36	−7.76	712.96	43.76	305.51	33.34	−136.17	−22.29	−823.75	−110.27	−270.11	−17.20	293.43	15.94
4	−415.44	−98.27	−424.85	−50.69	1026.76	81.29	−128.22	−54.26	31.40	8.61	−1225.58	−367.91	−261.23	−16.76	−4848.44	−266.41

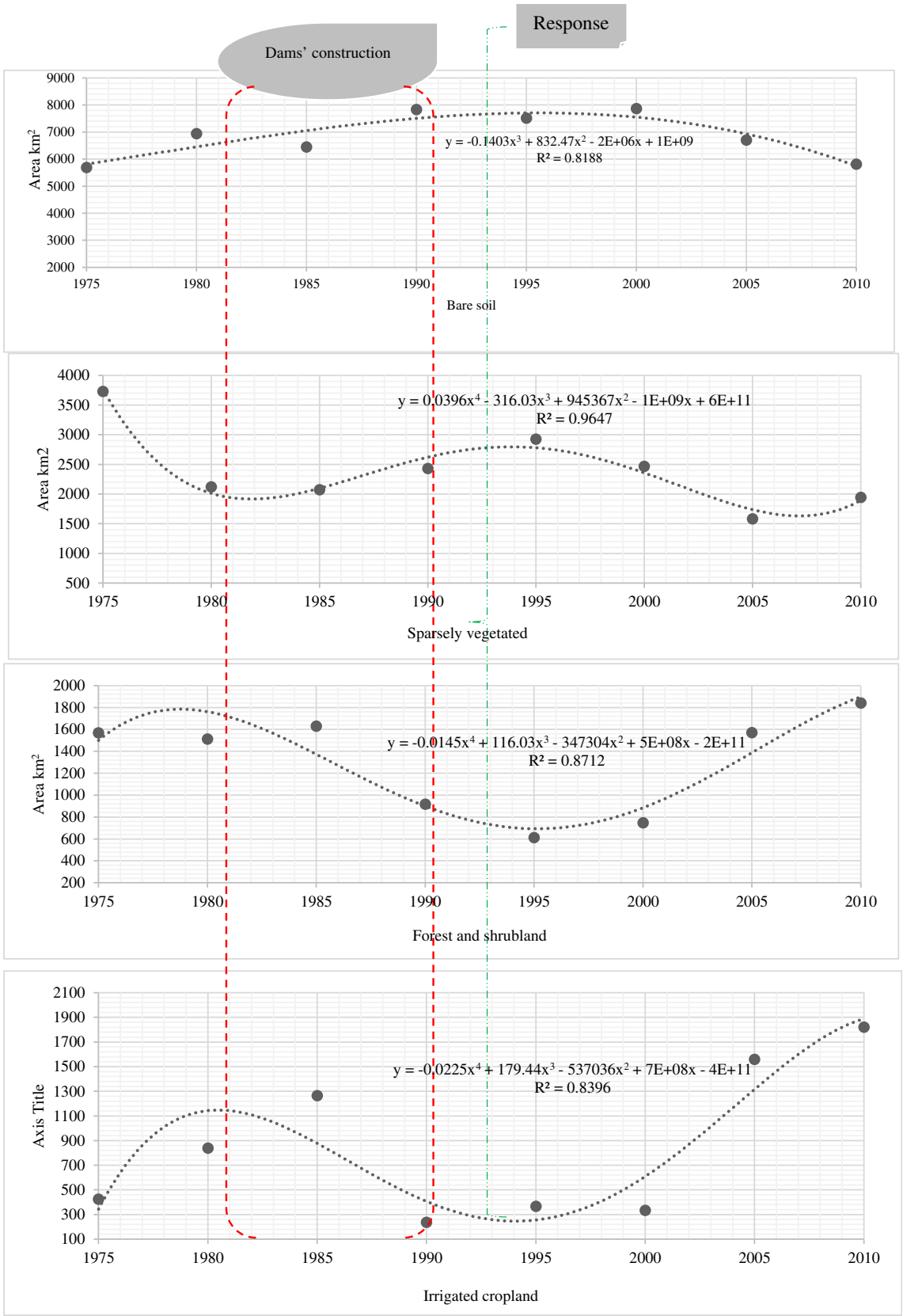

Fig. 4 Effect of dams' construction on spatial-temporal change of land cover

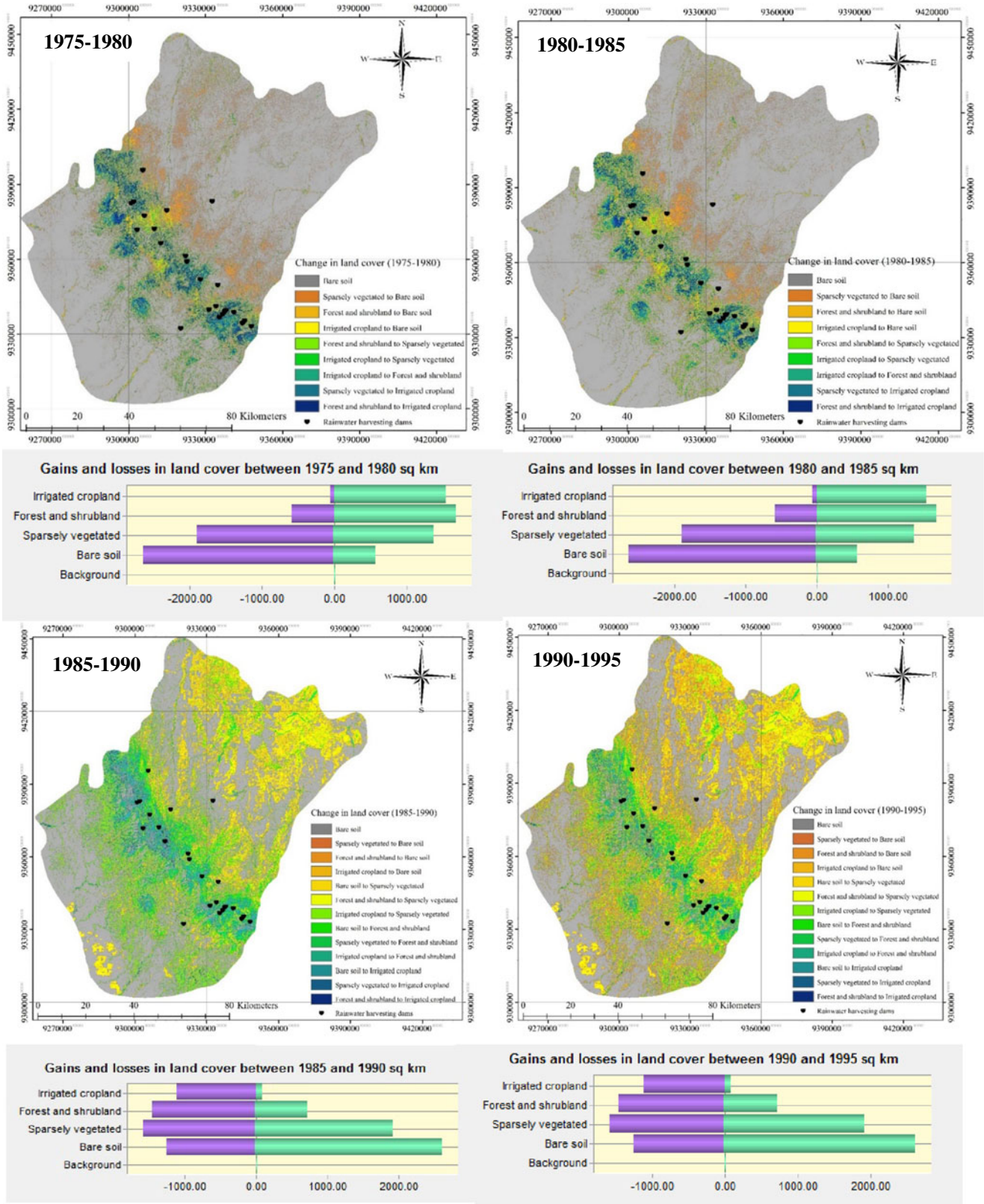

Fig. 5 Average change in land cover between each two time periods from 1975 to 1995

Mountains were largely removed and the remnants are further threatened by agricultural encroachment.

The environmental impacts of human activities induced LCC in arid regions has stimulated increased research in the

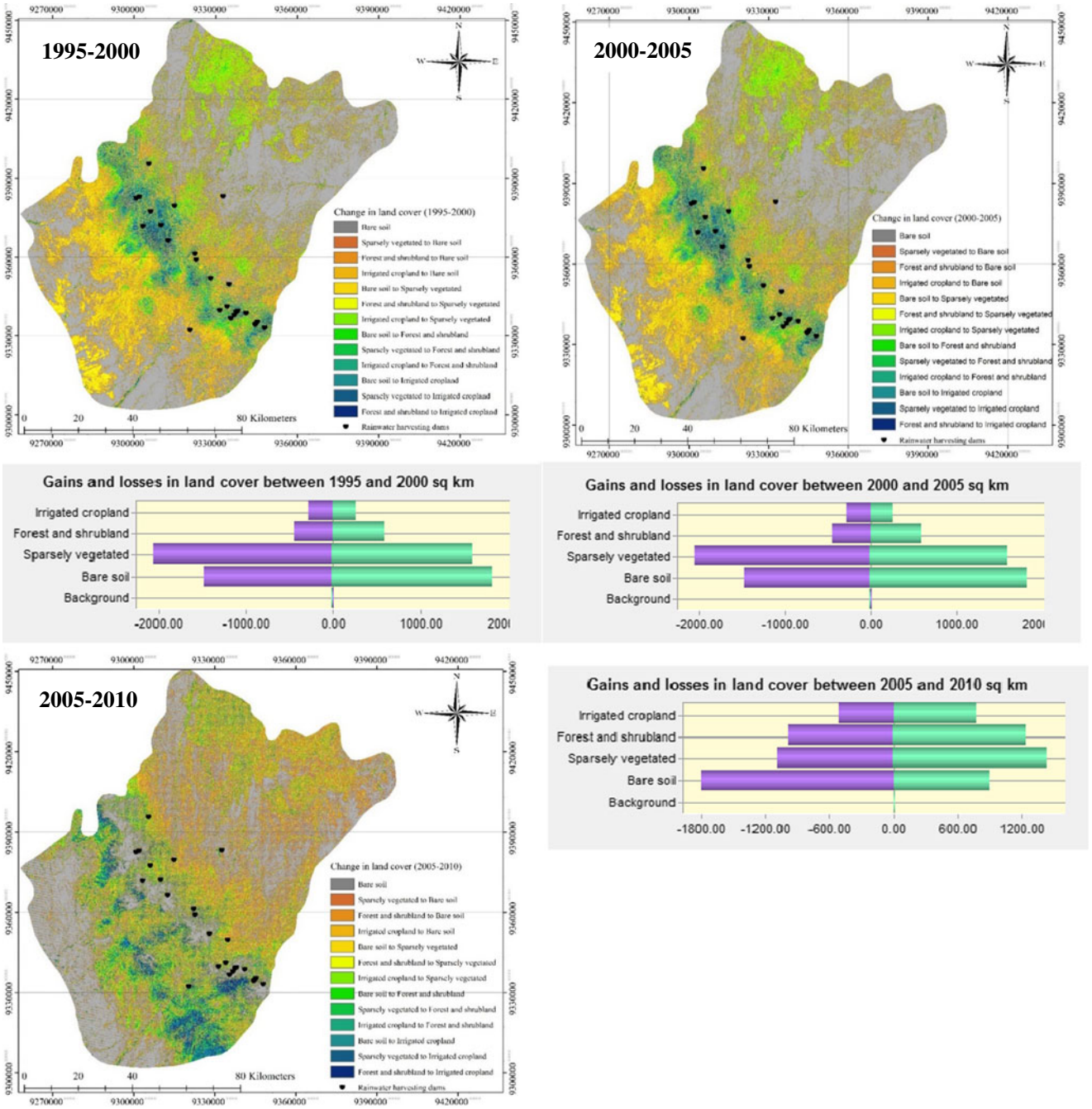

Fig. 6 Average change in land cover between each two time periods from 1995 to 2010

past few years due to the effects on water resources, climate, and ecosystem services. In the present study, the period and area selected were based on environmental concerns resulting from establishment of reservoirs and decreasing forest area. The analysis of LCC has revealed significant effects on the functioning of socioeconomic and environmental systems and important benefits for sustainability. This remarkable rate of LCC (forest and shrubland to irrigated cropland) raises many questions about environmental management and policy, driving forces of the agriculture growth process, ecosystem, forestry, land use and management policies followed, and sustainable environmental regulation implemented in the study area. This agricultural expansion occurred as a result of rapid increases in population and human activity and the establishment of large-scale water projects such as construction of dams and flood control infrastructures. Additionally, limited resource management resulted in the overexploitation of natural resources, with adverse effects on sustainable development. Land cover conversion has resulted in land degradation, interfered with biodiversity and the ecosystem, and caused

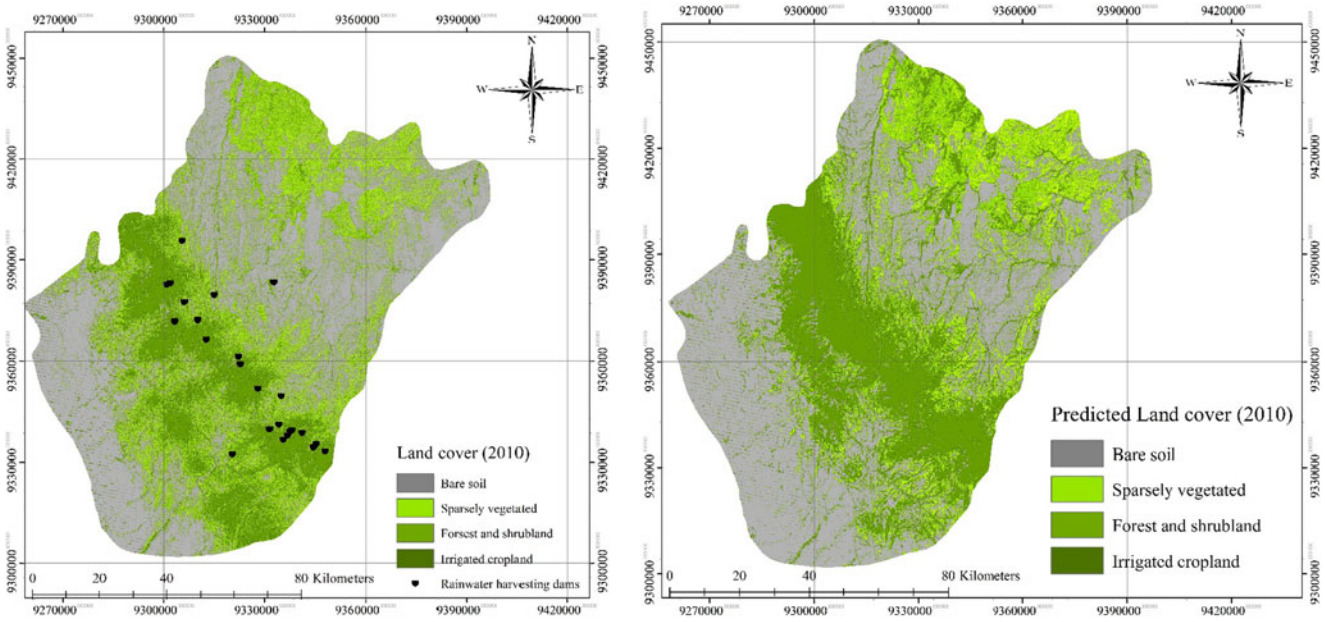

Fig. 7 Actual land cover map in 2010 (**a**) and predicted land cover in 2010 (**b**)

water stress in forest areas, thus depriving the region's wild animals of a much-needed source of water. Consequently, many wild animals have migrated to cities and villages in search of water and are fighting for their very survival, which may put human health and life at risk (Mahmoud and Alazba 2015).

Markov transition probability

The LC transition probabilities and transition area matrix for each two periods are calculated using Markov chain analysis as shown in Table 2. The diagonal of the transition probability represents the self-replacement probabilities, which is the probability of a LC class remaining the same or the probability of a change occurring from one LC class to another. The transition probabilities between 2000 and 2005 were used as input in the Markov-CA model. Markov chain analysis provided the capability of assembling transitions into a group of submodels and examining the potential power of explanatory variables. The projects from the change analysis were used to create the major transitions from areas that had more than 5 km^2. The earlier classified images and cross-classification images of each period were used to determine the relative frequency of different LC categories that occurred within the areas of transitions. The relative frequency and the distance from major transitions were used to test the driver variables, which were the different LC categories. Cramer's V was used to indicate the association between the variables and the major transitions. It is a "statistic measuring the strength of association or dependency between two (nominal) categorical variables" (Woo 2003). Variables that had Cramer's V of 0.4 or higher are good indicators of the major drivers of land transitions (Eastman 2006). The overall Cramer's V for the four classes ranged from 0.5 to 0.69, the highest values observed for bare soil and sparsely vegetated land as the main drivers for LCC.

Model validation and future land cover changes

The Markov-CA model was used to simulate the state of LC in 2000 and 2010 based on classified land cover maps in 1975, 1990, 2000, and 2005. The validation performed by the comparison of the mapped and simulated land cover categories for 2010 (Fig. 7). The validation result (Fig. 8) showed that the model successfully identified the state of land cover in 2000 and 2010 with 89.7 and 97 % agreement between the actual and projected cover, respectively. The model validation revealed that Markov-CA model successfully simulated bare soil, and forest and shrubland. These two categories obtained the best agreement between the simulated and actual areas, followed by sparsely vegetated land and irrigated cropland. Table 6 shows the extent of each land cover class in the simulated map and the actual map. For instance, in the actual map, bare soil was 5804 km^2 and the corresponding simulated category was 5728 km^2. Similarly, the measured area of forest and shrubland was 1840 km^2 and the simulated value was 1803 km^2. In general, Markov-CA model was able to predict land cover in 2010 (see Fig. 8).

Based on the success of the Markov-CA model to predict LC in 2010 using the 2000 and 2005 land cover. Markov-CA model was used to forecast the future land cover changes during the period of 2010–2050. The CA simulation predicts a continuing upward trend in irrigated cropland and forest and shrubland areas, as well as a downward trend in bare soil and

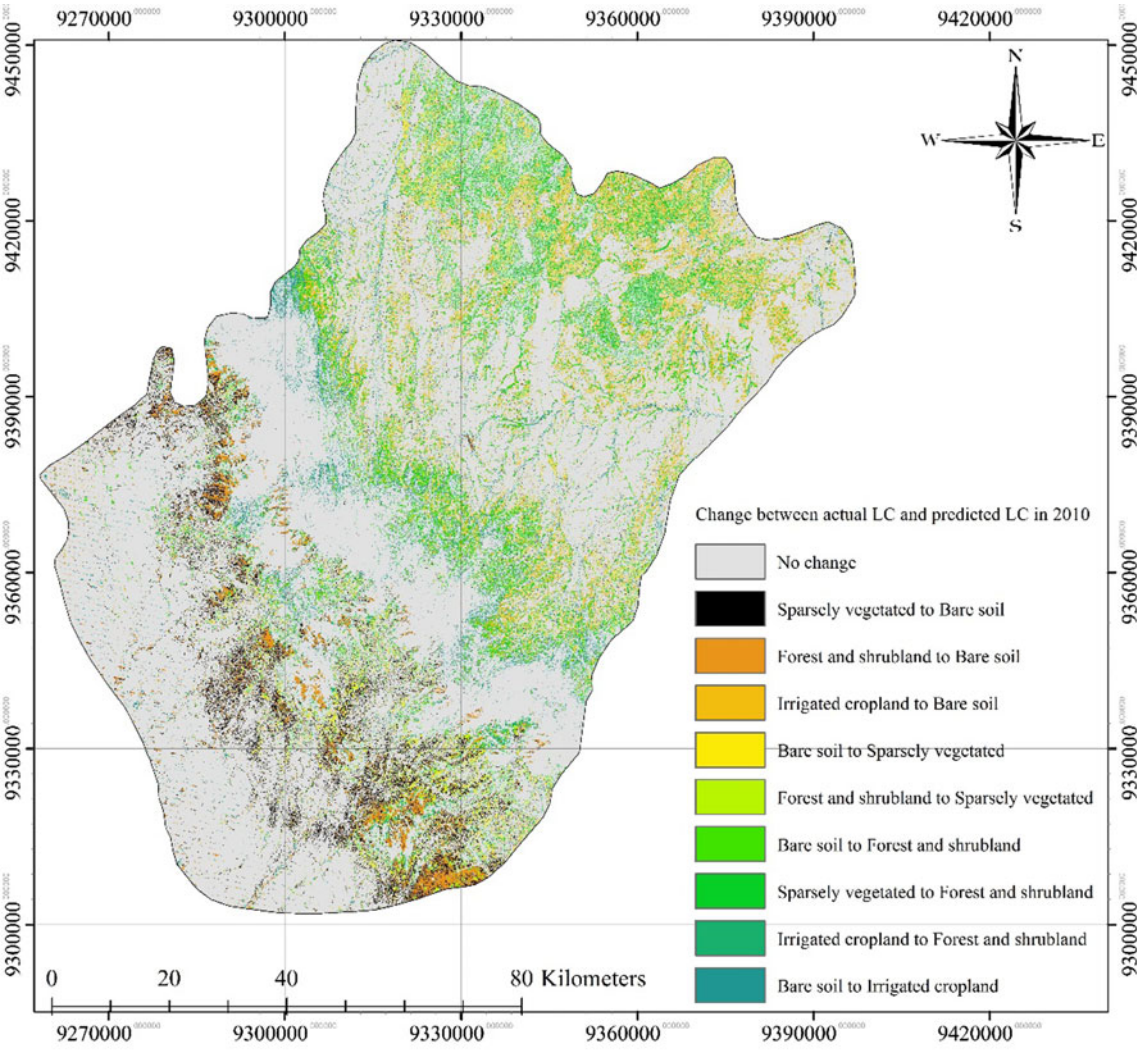

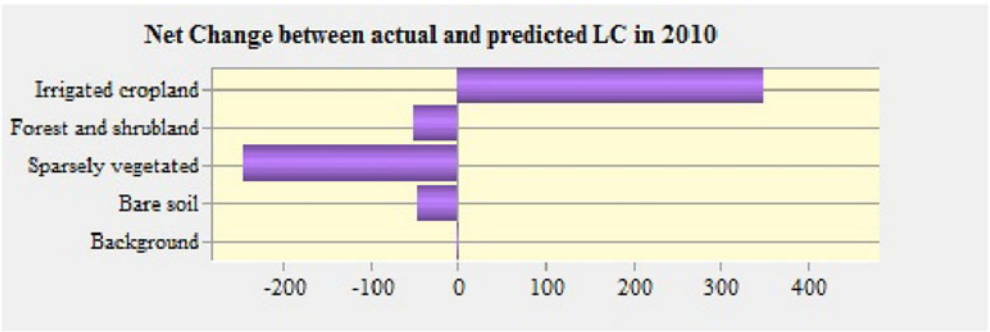

Fig. 8 Validation of predicted land cover in 2010

sparsely vegetated areas; the spatial distribution prediction indicates that irrigated cropland will expand around reservoirs and mountain areas. The projected land cover in 2050 (Fig. 9) shows a continued increase in irrigated cropland at the expense of forest and shrubland, which has significant environmental implications for the study area. The anticipated land cover distribution in 2050 is presented in Table 4 and Fig. 9. The projections show a dramatic drop in bare soil, from 5804 km^2 in 2010 to 2203 km^2 in 2050, and a similarly dramatic drop in sparsely vegetated land, which is predicted to decline from 1942 km^2 in 2010 to 988 km^2 in 2050. In contrast, forest and shrubland are likely to face a significant increase—a recovery caused by conservation plans, increasing from 840 km^2 in 2010 to more than 1547 km^2 in 2050—which is close to its value in 1975. Irrigated cropland is also slated to expand dramatically by 2050, being predicted to occupy an

Table 6 Observed and predicted area (km^2) per category of land cover

		2010 (measured)	2010 (predicted)
Code	Land cover class	Area (km^2)	Area (km^2)
1	Bare soil	5804.1	5728.4
2	Sparsely vegetated	1942.4	1710.5
3	Forest and shrubland	1840.9	1803.6
4	Irrigated cropland	1819.9	2164.9

Observed value was obtained from a GIS area calculation on the geometrically corrected satellite image. Area was predicted using Markov-CA chain analysis

area of 6668 km^2 instead of the 1819-km^2 area it occupied in 2010, a rise of 300 %. The results could encourage local governments, local residents, and farmers to address environmental problems in their regions. Further research can use this study to support an explanation of the linkages of land changes between water availability, human activities, and biophysical systems.

Due to the practical value of the results, the data and information generated during the analysis will be made available to local authorities. The output of this study would certainly be useful for decision makers and LC/land use planners in Saudi Arabia and similar arid regions to make appropriate planning and management of LC policies and its impact on the total environment in future. Land cover conversion in the studied area has resulted in land degradation, interfered with biodiversity and the ecosystem, and caused water stress in forest areas, thus depriving the region's wild animals of a much-needed source of water. Consequently, many wild animals have migrated to cities and villages in search of water and food creating substantial conflicts (Mahmoud and Alazba 2015). To avoid this, smart growth, which requires compact and environmentally friendly development, is encouraged for future land cover planning in Al-Baha region, KSA. Furthermore, the output of this study has the potential to help decision makers in arid areas to develop several important policies such as the following:

- Agriculture, forestry, land use and management policies
- Ecosystem services and life cycle assessments
- Environmental management and policies
- Human health risk assessment and management due to the imbalance caused by human activities

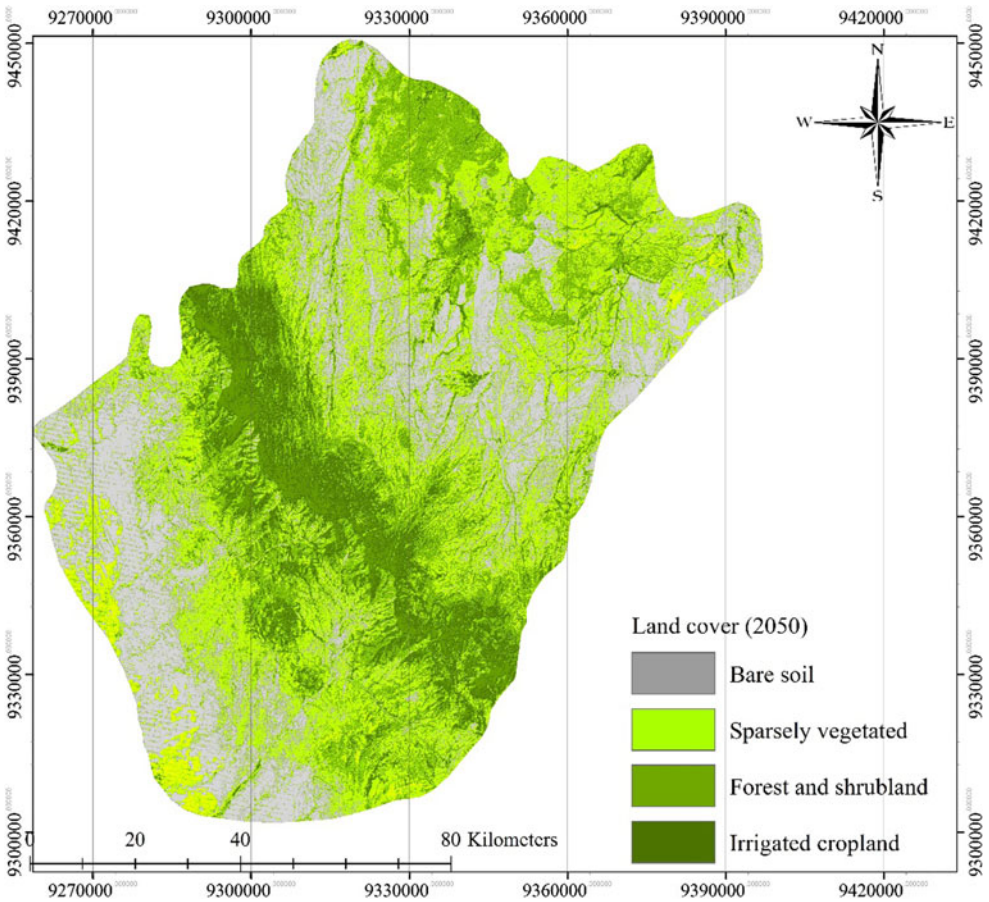

Fig. 9 Land cover projection in 2050

Conclusions

This study attempted to monitor and predict LCC in Al-Baha region, KSA, in addition to characterizing LCC and its dynamics by utilizing CA, remote sensing, and GIS techniques. Eight Landsat 5/7 TM/ETM images obtained for the years 1975, 1980, 1985, 1990, 1995, 2000, 2005, and 2010. These images incorporated with collected data from the specified region, and ultimately utilized in categorizing land cover. The LC maps are classified into four main classes: bare soil, sparsely vegetated, forest and shrubland, and irrigated cropland. Land cover change was quantified for the last 35 years within Al-Baha region, KSA, by the integration of Markov model and GIS. LC change was projected for the next 40 years using Markov chains and cellular automata. The classified images revealed four main classes: bare soil, sparsely vegetated land, forest and shrubland, and irrigated cropland. The images suggest that LCC have had a significant effect on forest and shrubland, which may have affected the ecosystem and natural balance of the study area.

The construction of rainwater-filled reservoirs affected the LC in the study area during the research period. In 1990, there was limited human interaction with the environment, and forest cover dominated the area. However, conditions changed significantly thereafter, and following reservoir construction, natural drainages were disrupted impacting native vegetation. Irrigated cropland underwent the greatest growth (from 422.8 km^2 in 1975 to 1819.9 km^2 in 2010) during the entire study period, and this agriculture expansion reached its peak in the 2000s.

A Markov-CA model was used to forecast the future LCC during the period of 2010–2050. The CA simulation predicts a continuing upward trend in irrigated cropland and forest, and shrubland areas, as well as a downward trend in bare soil and sparsely vegetated areas; the spatial distribution prediction indicates that irrigated cropland will expand around reservoirs and the mountain areas. The projected land cover in 2050 shows a continued increase in irrigated cropland at the expense of forest and shrubland, which has significant environmental implications for the study area. The projections show a dramatic drop in bare soil, from 5804 km^2 in 2010 to 2203 km^2 in 2050, and a similarly dramatic drop in sparsely vegetated land, which is predicted to decline from 1942 km^2 in 2010 to 988 km^2 in 2050. In contrast, forest and shrubland are likely to face a significant increase—a recovery caused by conservation plans, increasing from 840 km^2 in 2010 to more than 1547 km^2 in 2050—which is close to its value in 1975. Irrigated cropland is also planned to expand dramatically by 2050, being predicted to occupy an area of 6668 km^2 instead of the 1819 km^2 area it occupied in 2010, a rise of 300 %. Overall, the integration of CA and the Markov model offered a robust projection of land cover in 2050 and it is highly recommended to be used when prediction LCC with similar characteristics.

Acknowledgments This project received financial support from the King Saud University, Deanship of Scientific Research, College of Food and Agricultural Sciences Research Centre. The authors would like to thank Professor Boris Kondratieff, Colorado State University, Fort Collins, CO, USA, for his suggestions and linguistic assistance.

References

Abuelgasim AA, Ross WD, Woodcock CE (1999) Change detection using adaptive fuzzy neural networks. Remote Sens Environ 70(2):208–223

Alqurashi AF, Kumar L (2014) Land use and land cover change detection in the Saudi Arabian desert cities of Makkah and Al-Taif using satellite data. Adv Remote Sensing 3(03):106

Al-sharif, A. A., & Pradhan, B. (2013). Monitoring and predicting land use change in Tripoli Metropolitan City using an integrated Markov chain and cellular automata models in GIS. Arab J Geosci, 1–11.

Anderson, J., Hardy, E.E., Roach, J.T., and Witmer, R.E. (1976). A land use and land cover classification system for use with remote sensor data. US Geological Survey, Professional Paper 964.

Baker WL (1989) A review of models of landscape change. Landsc Ecol 2(2):111–133

Borrelli P, Sandia Rondón LA, Schütt B (2013) The use of Landsat imagery to assess large-scale forest cover changes in space and time, minimizing false-positive changes. Appl Geogr 41:147–157

Brown DG, Pijanowski BC, Duh JD (2000) Modeling the relationships between land use and land cover on private lands in the Upper Midwest, USA. Journal of. Environ Manag 59(4):247–263

Clarke KC, Gaydos LJ (1998). Loose-coupling a cellular automaton model and GIS: long-term urban growth prediction for San Francisco and Washington/Baltimore. Int J of Geogr Inf Sci 12(7):699–714

Clarke KC, Hoppen S, Gaydos L (1997) A self-modifying cellular automaton model of historical urbanization in the San Francisco Bay area. Environment and planning B: Planning and design 24(2):247–261

Clement F, Orange D, Williams M, Mulley C, Epprecht M (2009) Drivers of afforestation in Northern Vietnam: assessing local variations using geographically weighted regression. Appl Geogr 29(4):561–576

Dunjó G, Pardini G, Gispert M (2003) Land use change effects on abandoned terraced soils in a Mediterranean catchment, NE Spai*n*. *catena* 52:23–37

Eastman JR (2001) Guide to GIS and image processing Volume. Clark University, USA

Eastman, J. Ronald. 2006. IDRISI Andes: guide to GIS and image processing Massachusetts: Clark University.

Eastman JR, Fulk M (1993) Long sequence time series evaluation using standardized principle components. Photogramm. Eng. Rem. Sens. 59:991–996

Elatawneh A, Kalaitzidis C, Petropoulos GP, Schneider T (2014) Evaluation of diverse classification approaches for land use/cover mapping in a Mediterranean region utilizing Hyperion data. Int J Digital Earth 7(3):194–216

Guan D, Li H, Inohae T, Su W, Nagaie T, Hokao K (2011) Modeling urban land use change by the integration of cellular automaton and Markov model. Ecol Model 222(20):3761–3772

Haregeweyn N, Fikadu G, Tsunekawa A, Tsubo M, Meshesha DT (2012) The dynamics of urban expansion and its impacts on land use/land cover change and small-scale farmers living near the urban fringe: a case study of Bahir Dar, Ethiopia. Landsc Urban Plan 106(2):149–157

Heistermann M, Müller C, Ronneberger K (2006) Land in sight? Achievements, deficits and potentials of continental to global scale land-use modeling. Agric Ecosyst Environ 114:141–158

Hereher ME, Al-Shammari AM, Allah SEA (2012) Land Cover Classification of Hail—Saudi Arabia Using Remote Sensing. Int J Geosci 3(02):349

Huang Q, He C, Liu Z, Shi P (2014) Modeling the impacts of drying trend scenarios on land systems in northern China using an integrated SD and CA model. Sci China Earth Sci 57(4):839–854

Huishi D, Eerdun H, Yi Y, Jing A (2012) Land coverage changes in the Hulun Buir grassland of China based on the cellular automata-Markov model. International Proceedings of Chemical, Biological & Environmental Engineering, pp. 69–74

Jensen JR (2005) Introductory digital image processing: a remote sensing perspective, 3rd edn. Prentice Hall, Inc., Upper Saddle River, N.J., 526 pp

Kamusoko C, Aniya M, Adi B, Manjoro M (2009) Rural sustainability under threat in Zimbabwe—simulation of future land use/cover changes in the Bindura district based on the Markov-cellular automata model. Appl Geogr 29(3):435–447

Kashaigili JJ, Majaliwa AM (2010) Integrated assessment of land use and cover changes in the Malagarasi river catchment in Tanzania. Phys Chem Earth, Parts A/B/C 35(13):730–741

Lambin EF (1997) Modeling and monitoring land-cover change processes in tropical regions. Progress in Phys. Geography 21(3):375–393

Li Z, Liu W, Wang Q (2008) Effects of land use type and slope position on soil physical properties in loess tableland area. Yingyong Shengtai Xuebao 19:1303–1308

Li Z, Liu W-Z, Zhang X-C, Zheng F-L (2009) Impacts of land use change and climate variability on hydrology in an agricultural catchment on the Loess Plateau of China. J Hydrol 377:35–42

Liu Y, Dai L, Xiong H (2014) Simulation of urban expansion patterns by integrating auto-logistic regression. Markov chain and cellular automata models. J Environ Plan Manage. doi:10.1080/09640568.2014.916612

Long H, Tang G, Li X, Heilig GK (2007) Socio-economic driving forces of land-use change in Kunshan, the Yangtze River Delta economic area of China. J Environ Manag 83(3):351–364

Longley P, Batty M (eds) (1996) Spatial analysis: modelling in a GIS environment. GeoInformation International, Cambridge. 0-470-23615-9

Longley PA, Goodchild MF, Maguire DJ (eds) (2005) Geographic information systems and science. John Wiley & Sons, Ltd., Chichester

López E, Bocco G, Mendoza M, Duhau E (2001) Predicting land-cover and land-use change in the urban fringe: a case in Morelia city, Mexico. Landsc Urban Plan 55(4):271–285

Lu D, Mausel P, Brondízio E, Moran E (2004) Change detection techniques. Int J Remote Sens 25(12):2365–2407

Madugundu R, Al-Gaadi KA, Patil VC, Tola E (2014) Detection of land use and land cover changes in Dirab region of Saudi Arabia using remotely sensed imageries. Am J Environ Sci 10(1):8

Mahmoud SH, Alazba AA (2015) Hydrological response to land cover changes and human activities in arid regions using a geographic information system and remote sensing. PLoS One 10(4): e0125805. doi:10.1371/journal.pone.0125805

Mahmoud SH (2014) Delineation of potential sites for groundwater recharge using a GIS-based decision support system. Environ Earth Sci. doi:10.1007/s12665-014-3249-y

Mahmoud SH, Alazba AA, Amin MT (2014a) Identification of potential sites for groundwater recharge using a GIS-based decision support system in Jazan region-Saudi Arabia. Water Resour Manag 28(10): 3319–2240

Mahmoud SH, Alazba AA (2014) The potential of in situ rainwater harvesting in arid regions: developing a methodology to identify suitable areas using GIS-based decision support system. Arab J Geosci. doi:10.1007/s12517-014-1535-3

Mahmoud SH, Mohammad FS, Alazba AA (2014b) Delineation of potential sites for rainwater harvesting structures using a geographic information system-based decision support system. Hydrology Research. doi:10.2166/nh.2014.054

Mahmoud SH, Mohammad FS, Alazba AA (2014c) Determination of potential runoff coefficient for Al-Baha region, Saudi Arabia. Arab J Geosci 7(5):2041–2057

Marey-Pérez MF, Rodríguez-Vicente V (2009) Forest transition in Northern Spain: local responses on large-scale programmes of field-afforestation. Land Use Policy 26(1):139–156

Marshall E, Randhir TO (2008) Spatial modeling of land cover change and watershed response using Markovian cellular automata and simulation. Water Resour Res 44(4)

Milesi C, Hashimoto H, Running SW, Nemani RR (2005) Climate variability, vegetation productivity and people at risk. Glob Planet Chang 47:221–231

Mitsova D, Shuster W, Wang X (2011) A cellular automata model of land cover change to integrate urban growth with open space conservation. Landsc Urban Plan 99(2):141–153

Myint SW, Wang L (2006) Multicriteria decision approach for land use land cover change using Markov chain analysis and a cellular automata approach. Can J Remote Sens 32(6):390–404

Nouri J, Gharagozlou A, Arjmandi R, Faryadi S, Adl M (2011) Predicting urban land use changes using a CA–Markov model. Arab J Sci Eng 39:5565–5573

Pastor J, Bonde J, Johnston C, Naiman RJ (1993) Markovian analysis of the spatially dependent dynamics of beaver ponds. In Gardner RH (ed) Predicting spatial effects in ecological systems. Lectures on mathematics in the life sciences, vol 23. American Mathematical Society, Providence, pp 5–27

Petropoulos GP, Kalaitzidis C, Vadrevu KP (2012) Support vector machines and object-based classification for obtaining land-use/cover cartography from Hyperion hyperspectral imagery. *Comput Geosci* 41:99–107

Petropoulos GP, Kontoes C, Keramitsoglou I (2011) Burnt area delineation from a uni-temporal perspective based on Landsat TM imagery classification using support vector machines. Int J Appl Earth Obs Geoinf 13(1):70–80

Petropoulos GP, Vadrevu KP, Xanthopoulos G, Karantounias G, Scholze M (2010) A comparison of spectral angle mapper and artificial neural network classifiers combined with Landsat TM imagery analysis for obtaining burnt area mapping. Sensors 10(3):1967–1985

Petrosillo, I., Semeraro, T., Zaccarelli, N., Aretano, R., & Zurlini, G. (2013). The possible combined effects of land-use changes and climate conditions on the spatial–temporal patterns of primary production in a natural protected area. Ecol Indic, 29, 367–375.

Pontius RG Jr (2000) Quantification error versus location error in comparison of categorical maps. Photogramm Eng Remote Sensing 66(8):1011–1016

Pontius GR, Malanson J (2005) Comparison of the structure and accuracy of two land change models. Int J Geogr Inf Sci 19:243–265

Redo D, Joby Bass JO, Millington AC (2009) Forest dynamics and the importance of place in western Honduras. Appl Geogr 29(1)

Richards JA (1999) Remote sensing digital image analysis (Vol. 3). Berlin et al.: Springer.

Ridd M, Liu J (1998) A comparison of four algorithms for change detection in an urban environment. Remote Sens Environ 63:95–100

Roy, H. G., Fox, D. M., & Emsellem, K. (2014). Predicting land cover change in a Mediterranean catchment at different time scales. In Computational science and its applications–ICCSA 2014 (pp. 315–330). Springer International Publishing.

Satake A, Rudel T (2007) Modeling the forest transition: forest scarcity and ecosystem service hypotheses. Ecol Appl 17(7):2024–2036

Shoyama K, Yamagata Y (2014) Predicting land-use change for biodiversity conservation and climate-change mitigation and its effect on

ecosystem services in a watershed in Japan. Ecosystem Services. doi:10.1016/j.ecoser.2014.02.004

Srivastava PK, Han D, Rico-Ramirez MA, Bray M, Islam T (2012) Selection of classification techniques for land use/land cover change investigation. Adv Space Res 50(9):1250–1265

Teferi E, Bewket W, Uhlenbrook S, Wenninger J (2013) Understanding recent land use and land cover dynamics in the source region of the Upper Blue Nile, Ethiopia: Spatially explicit statistical modeling of systematic transitions. Agric Ecosyst Environ 165:98–117

Tong ST, Sun Y, Ranatunga T, He J, Yang YJ (2012) Predicting plausible impacts of sets of climate and land use change scenarios on water resources. Appl Geogr 32(2):477–489

Torrens, P. M. (2003). Automata-based models of urban systems. Advanced spatial analysis, 61–79.

Townshend JRG (1981) Terrain analysis and remote sensing. George Allen and Unwin, London

Turner BL, Meyer WB, Skole DL (1994) Global land-use land-cover change –towards an integrated study. Ambio 23(1):91–95

Turner BL, Lambin EF, Reenberg A (2007) the emergence of land change science for global environmental change and sustainability. Proceed Natl Acad Sci (PNAS) 104(52):20666–20671

Turner, B.L., Moss, R.H., Skole, D.L., 1993. Relating land-use and global land-cover change: a proposal for an IGBP-HDP core project. Global Change IGBP No. 24, HDP report No. 5.

Wagner DF (1997) Cellular automata and geographic information systems. Environ Plan B 24(2):219–234

Wang H, Li X, Long H, Gai Y, Wei D (2009) Monitoring the effects of land use and cover changes on net primary production: A case study in China's Yongding River basin. For Ecol Manag 258(12):2654–2665

White R, Engelen G, Uljee I (1997) The use of constrained cellular automata for high- resolution modeling of urban land use dynamics. Environ Plan B 24:323–343

Wilson CO, Weng Q (2011) Simulating the impacts of future land use and climate changes on surface water quality in the Des Plaines River watershed, Chicago Metropolitan Statistical Area, Illinois. Sci Total Environ 409(20):4387–4405

Woo, Chi. (2003). Cramer's V http://planetmath.org/encyclopedia/CramersV.html. (Accessed June 25, 2013).

Yagoub MM, Al Bizreh AA (2014) Prediction of land cover change using Markov and cellular automata models: case of Al-Ain, UAE, 1992-2030. J Indian Soc Remote Sensing 42(3):665–671

Yao C, Chang L, Ding J, Li Z, An D, Zhang Y (2014) Evaluation of the effects of underlying surface change on catchment hydrological response using the HEC-HMS model. Proceed Int Assoc Hydrological Sci 364:145–150

Zhang J, Zhengjun L, Xiaoxia S (2009) Changing landscape in the Three Gorges Reservoir Area of Yangtze River from 1977 to 2005: Land use/land cover, vegetation cover changes estimated using multi-source satellite data. Int J Appl Earth Obs Geoinf 11(6):403–412

Zhang WW, Yao L, Li H, Sun DF, Zhou LD (2011) Research on land use change in Beijing Hanshiqiao Wetland Nature Reserve using remote sensing and GIS. Procedia Environ Sci 10:583–588

Vorovencii I, Muntean DM (2012) Evaluation of supervised classification algorithms for Landsat 5 TM images. RevCAD J Geodesy Cadastre 11(1):229–238